J Mater Sci (2011) 46:4005–4012
DOI 10.1007/s10853-011-5328-8

Two novel propylenedioxythiophene-based copolymers with donor–acceptor structures for organic solar cell materials

Zheng Wang · Feng Tao · Long-yi Xi · Kai-ge Meng · Wei Zhang · Ying Li · Qing Jiang

Received: 16 November 2010 / Accepted: 24 January 2011 / Published online: 8 February 2011

Abstract Two novel conjugated copolymers consisting of alternating electron-rich propylenedioxythiophene and electron-deficient 2,3-diphenyltheno[3,4-b]pyrazine or 6,7-diphenyl[1,2,5]thiadiazole units have been synthesized through palladium catalyzed Sonogashira triple-bond coupling reaction. The structures and properties of the two copolymers, $\mathbf{P_1}$, $\mathbf{P_2}$, were characterized by FT-IR, NMR, UV–Vis absorbance (Abs), thermal gravimetric analysis (TGA), differential scanning calorimetry (DSC), and cyclic voltammetry (CV). UV–Vis absorption spectra of the polymers show two absorption bands both in $CHCl_3$ solution and films. The absorption peak maxima of $\mathbf{P_1}$, $\mathbf{P_2}$ are 600 nm, 766 nm in solution and 627 nm, 823 nm in films, respectively. Thermal gravimetric analysis demonstrates that the two polymers are stable below 300 °C. Cyclic voltammetry studies reveal that the band gaps of $\mathbf{P_1}$, $\mathbf{P_2}$ are 1.62 eV and 1.50 eV, suggesting their potential for applications as organic solar cell materials.

Introduction

Harvesting energy directly from sunlight using photovoltaic technology is one of the most important ways to address the growing global energy needs. Polymer solar cells (PSCs) are becoming a promising alternative for clean and renewable energy due to their unique advantages, such as light weight, low cost, and processability [1–8]. However, PSCs are, in general, of low efficiency compared to their inorganic counterparts due to their relatively narrow absorption bands and large band gaps [9–13].

A facile approach to achieve low band-gap polymers is through incorporation of electron-rich unit (as donor) and electron-deficient unit (as acceptor), forming a donor–acceptor (D–A) structure. Through the push–pull interaction, efficient photoinduced intramolecular charge transfer takes place from the donor to the acceptor, generating an absorption band at the lower energy [14–20]. The band gaps and energy levels of these conjugated polymers can be easily tuned by selecting different electron-rich and electron-deficient units.

The use of heteroaromatic fused-ring derivative, including propylenedioxythiophene unit as donor has established an interesting approach to create π-conjugated polymers that provide enhanced photovoltaic properties [21–25]. These fused ring systems enhance coplanarity, which is beneficial for the π-conjugation, and enable closer interchain interactions that are generally considered to be beneficial for charge transport. However, up to now, most of the propylenedioxythiophene-based copolymers were synthesized by single-bond or double-bond polycondensation [26–31]. These methods could not keep the target copolymers coplanarity or linearity to the greatest extent. So in this work, we have studied and synthesized two novel copolymers based on alternating electron-rich propylenedioxythiophene and electron-deficient 2,3-diphenyltheno[3,4-b]pyrazine or 6,7-diphenyl[1,2,5]thiadiazole units through palladium catalyzed Sonogashira triple-bond condensation polymerization.

The long alky chains on the propylenedioxythiophene could enhance the solubility of the copolymers. The incorporation of triple-bond into the copolymer backbones can be as one approach to enhance π-electron delocalization to match well to the solar spectrum. Herein, we report

Z. Wang · F. Tao · L. Xi · K. Meng · W. Zhang · Y. Li (✉) · Q. Jiang
College of Chemistry, Sichuan University, Chengdu 610064, China
e-mail: profliying@sina.com

our initial results of synthesis, characterization, thermal, optical and electrochemical properties of the two novel copolymers.

Experimental

Materials

All reagents were purchased from Aldrich or Acros Chemical companies and were used without further purification. All the solvents were purified according to the standard methods prior to use. 2,3-Diphenyltheno[3,4-b]pyrazine (**10**) [32, 33] and 6,7-diphenyl[1,2,5]thiadiazole (**11**) [34–36] were prepared according to the similar procedures reported.

Synthesis of monomers

*Dioctylmalonate (**1**)*

To a 250 mL flame dried three-neck round bottom flask equipped with an argon inlet, 150 mL of dry THF, 21.6 g (112 mmol) of octyl bromide, and 4.50 g (112 mmol) of NaH were added. The flask was cooled to 0 °C in an ice bath and 5.70 mL (37.4 mmol) of fresh distilled diethyl malonate was added dropwise through the addition funnel. When the addition of the malonate was completed, the mixture was refluxed 12 h. The flask was then cooled to 0 °C in an ice bath and the remaining NaH was quenched by adding water dropwise. The mixture was then poured into brine (200 mL), extracted with ethyl acetate three times, washed with brine. The combined organic layer was dried over $MgSO_4$. The solvent and the octyl bromide were removed under vacuum. The crude oil obtained was then used in the next step without further purification.

*2,2-Dioctylpropane-1,3-diol (**2**)*

To a 250 mL flame dried three-neck round-bottom flask equipped with an argon inlet, 150 mL of dry ethyl ether and 3.80 g (100 mmol) of $LiAlH_4$ powder were added. The crude dioctyl malonate (**1**) 9.70 g (25.0 mmol) was added dropwise at 0 °C in an ice bath. When the addition was completed, the mixture was allowed to warm to room temperature. The reaction mixture was stirred under argon for 20 h. The flask was then cooled to 0 °C in an ice bath again and the remaining $LiAlH_4$ was quenched by adding water dropwise. The solid residue was filtered; the filtrate was extracted with ethyl acetate three times, washed with brine. The combined organic layer was dried over $MgSO_4$. After removal the solvent under reduced pressure, the residue was purified by column chromatography on silica gel (petroleum ether/ethyl acetate, v/v, 2/1) to give a white solid **2** (3.60 g, 48.2%). ^{1}H-NMR (400 MHz, $CDCl_3$, δ): 3.58 (s, 4H), 2.13 (s, 2H), 1.23–1.32 (m, 28H), 0.86–0.90 (m, 6H).

*2,3,4,5-Tetrabromothiophene (**3**)*

Bromine (15.1 g, 190 mmol) was added dropwise with temperature maintained at 10–15 °C to thiophene (4.00 g, 47.0 mmol) in chloroform (6 mL) and stirred. When the addition of the bromine was completed, reaction mixture was continued for stirring at room temperature for 2 h, and then heated to reflux for 16 h. The reaction mixture was poured into the solution of sodium hydroxide to quench the excess of bromine and washed with water several times to get a white solid **3** (16.8 g, 85.1%). M.p: 80–82 °C. ^{1}H-NMR (400 MHz, $CDCl_3$, δ): No proton was observed.

*3,4-Dibromothiophene (**4**)*

2,3,4,5-Tetrabromothiophene (**3**) (5.00 g, 12.6 mmol) was added to the mixture of glacial acetic acid (8 mL) and water (2 mL) followed by slow addition of zinc (4.90 g, 75.6 mmol). The reaction mixture was kept for stirring at room temperature for 12 h. The remaining zinc was filtered; the filtrate was extracted with ethyl acetate, washed with brine repeatedly. The combined organic layer was dried over $MgSO_4$. After removal the solvent under reduced pressure, the residue was purified by column chromatography on silica gel (petroleum ether) to give a colorless liquid **4** (2.60 g, 87.3%). ^{1}H-NMR (400 MHz, $CDCl_3$, δ): 7.31 (d, $J = 3.6$ Hz, 2H).

*3,4-Dimethoxythiophene (**5**)*

Sodium metal (2.20 g, 93.4 mmol) was taken in a 100 mL three-neck round-bottom flask and dry methanol (25 mL) was added to it dropwise. 3,4-Dibromothiophene (**4**) (2.50 g, 10.4 mmol) was added to it followed by the addition of cupric oxide (0.55 g, 6.90 mmol) and potassium iodide (0.17 g, 1.04 mmol). The mixture was stirred at 80 °C for 48 h. The reaction mixture was poured into cold water and extracted with ethyl acetate, washed with water repeatedly, dried over $MgSO_4$. After removal the solvent under vacuum, the crude product was purified by column chromatography on silica gel (petroleum ether/dichloromethane, v/v, 3/1) to give a colorless liquid **5** (0.75 g, 50.0%). ^{1}H-NMR (400 MHz, $CDCl_3$, δ): 6.19 (s, 2H), 3.86 (s, 6H).

*3,4-Dihydro-3,3-dioctyl-2H-thieno[3,4-b][1,4]dioxepine (**6**)*

3,4-Dimethoxythiophene (**5**) (0.25 g, 1.74 mmol), 2,2-dioctylpropane-1,3-diol (**2**) (0.60 g, 2.00 mmol), *p*-toluenesulfonic

acid (0.034 g, 0.170 mmol), and 60 mL of dry toluene were combined in a 150 mL flask equipped with a Soxhlet extractor with $CaCl_2$ in a cellulose thimble. The solution was refluxed for 48 h. The reaction mixture was cooled and washed once with water. The toluene was removed under vacuum, and the crude product was purified by column chromatography on silica gel (petroleum ether/dichloromethane, v/v, 10/1) to give a colorless liquid **6** (0.36 g, 54.5%). ^{1}H-NMR (400 MHz, $CDCl_3$, δ): 6.43 (s, 2H), 3.86 (s, 4H), 1.38 (m, 4H), 1.25–1.32 (m, 24H), 0.89 (m, 6H).

*6,8-Dibromo-3,4-dihydro-3,3-dioctyl-2H-thieno[3,4-b][1,4]dioxepine (**7**)*

To a 250 mL three-neck round-bottom flask, 3,4-dihydro-3,3-dioctyl-2H-thieno[3,4-b][1,4]-dioxepine (**6**) (0.56 g, 1.47 mmol) was dissolved in 100 mL dry DMF. NBS (0.65 g, 3.68 mmol) with 20 mL DMF was added dropwise through the addition funnel and the reaction was stirred for 5 h at room temperature under argon. Water (100 mL) was added to the reaction and the aqueous phase was extracted with ethyl acetate three times, washed with brine repeatedly. The combined organic layer was dried over $MgSO_4$. After solvent evaporation, the resulting oil was purified by column chromatography on silica gel (petroleum ether/dichloromethane, v/v, 10/1) to give a colorless liquid **7** (0.67 g, 84.2%). ^{1}H-NMR (400 MHz, $CDCl_3$, δ): 3.83 (s, 4H), 1.46 (m, 4H), 1.24–1.32 (m, 24H), 0.80 (m, 6H).

*6,8-Diethynyl-bis(3-hydroxy-3-methyl-1-butynyl)-3,3-dioctyl-3,4-dihydro-2H-thieno[3,4-b][1,4]-dioxepine (**8**)*

To a 100 mL three-necked flask, 6,8-dibromo-3,4-dihydro-3,3-dioctyl-2H-thieno[3,4-b][1,4]-dioxepine (**7**) (0.50 g, 0.93 mmol), Pd $(PPh_3)_2Cl_2$ (3.1 mg), CuI (5 mg), PPh_3 (15 mg) were added, the mixture was degassed with nitrogen three times. In addition, $N(Et)_3$ (30 mL) was degassed at room temperature for 1 h and injected into the mixture, and then 2-methyl-3-butyn-2-ol (0.32 g, 3.72 mmol) was injected. The mixture was heated to 70 °C standing for 5 h, cooled to room temperature, and poured into water, extracted three times with methylene chloride. All organic layers were combined, washed with water, and dried over $MgSO_4$. After solvent evaporation, the resulting oil was purified by column chromatography on silica gel (petroleum ether/ethyl acetate, v/v, 4/1) to give a colorless liquid **8** (0.37 g, 73.6%). ^{1}H-NMR (400 MHz, $CDCl_3$, δ): 3.90 (s, 4H), 2.17 (s, 2H), 1.59 (s, 12H), 1.27–1.36 (m, 28H), 0.88 (m, 6H).

*6,8-Diethynyl-3,3-dioctyl-3,4-dihydro-2H-thieno-[3,4-b][1,4]dioxepine (**9**)*

To a 100 mL three-necked flask, a mixture of 6,8-diethynyl-bis(3-hydroxy-3-methyl-1-butynyl)-3,3-dioctyl-3,4-dihydro-2H-thieno[3,4-b][1,4]-dioxepine (**8**) (0.85 g, 1.56 mmol) and KOH (0.35, 6.25 mmol) in 40 mL of toluene was heated refluxed under N_2 with a vigorous stirring for 5 h. The solvent was then removed and the crude product was purified by column chromatography on silica gel (petroleum ether) to give a colorless liquid **9** (0.42 g, 62.4%). ^{1}H-NMR (400 MHz, $CDCl_3$, δ): 3.89 (s, 4H), 3.38 (s, 2H), 1.18–1.37 (m, 28H), 0.81–0.88 (m, 6H). ^{13}C-NMR (400 MHz, $CDCl_3$, δ): 151.9, 102.4, 84.5, 74.5, 43.8, 32.0, 31.7, 30.4, 29.7, 29.4, 22.7, 21.3, 19.7, 14.1.

Synthesis of polymers

General procedure: 6,8-diethynyl-3,3-dioctyl-3,4-dihydro-2H-thieno[3,4-b][1,4]dioxepine (**9**) (1.0 mmol), 2,3-diphenylthieno[3,4-b]pyrazine (**10**) or 6,7-diphenyl[1, 2, 5]thiadiazole (**11**) (1.0 mmol), Pd $(PPh_3)_2Cl_2$ (0.0876 mmol), CuI (0.333 mmol) and PPh_3 (0.48 mmol) were added to a 25 mL three-necked flask and the mixture was degassed with nitrogen three times. In addition, toluene (10 mL) and 2 mol/L K_2CO_3 (5.0 mL) were degassed at room temperature for 1 h and injected into the mixture, respectively. The reaction was then stirred to 100 °C for 6 h and the reactant was poured into 200 mL methanol, after stirring for 30 min, the precipitate was collected and washed repeatedly with water. The residue was dissolved in $CHCl_3$, filtered, poured into methanol again, the precipitate was then Soxhlet extracted with acetone for 8 h. The copolymer was collected by filtration and dried under vacuum.

P_1: Dark blue solid. IR (KBr pellet, cm^{-1}): 3442, 2923, 2852, 2851, 2173, 1630, 1440, 1371, 1262, 1062, 804, 767, 695. ^{1}H-NMR (400 MHz, $CDCl_3$, δ): 7.65–7.69 (m, 2H), 7.46–7.56 (m, 4H), 7.31–7.37 (m, 4H), 4.02–4.06 (m, 4H), 1.08–1.68 (m, 28H), 0.78–0.89 (m, 6H). ^{13}C-NMR (400 MHz, $CDCl_3$, δ): 154.1, 151.8, 142.9, 138.7, 133.1, 132.1, 131.9, 130.1, 129.2, 128.5, 128.1, 115.7, 104.7, 92.7, 89.3, 43.9, 39.4, 37.4, 37.1, 32.7, 32.2, 31.9, 30.1, 29.7, 29.5, 29.3, 28.0, 27.1, 26.4, 24.5.

P_2: Dark green solid. IR (KBr pellet, cm^{-1}): 3439, 2850, 2165, 1645, 1441, 1370, 1257, 1059, 899, 797, 760, 692. ^{1}H-NMR (400 MHz, $CDCl_3$, δ): 7.65–7.69 (m, 4H), 7.53–7.55 (m, 2H), 7.44–7.49 (m, 4H), 3.95–3.98 (m, 4H), 1.22–1.68 (m, 28H), 0.86–0.92 (m, 6H). ^{13}C-NMR (400 MHz, $CDCl_3$, δ): 156.0, 140.4, 132.1, 128.4, 121.2, 116.0, 107.2, 90.7, 42.3, 39.6, 37.4, 33.8, 31.9, 29.6, 29.4, 29.3, 22.6, 14.1.

Results and discussion

Synthesis and characterization

The general synthetic routes toward the monomers are depicted in Scheme 1. The polymerization of $\mathbf{P_1}$ and $\mathbf{P_2}$ are depicted in Scheme 2. Alternating copolymer $\mathbf{P_1}$ and $\mathbf{P_2}$ were prepared by the Sonogashira coupling reaction with 1:1 monomer ratio in the presence of $Pd(PPh_3)_2Cl_2$ as catalyst and CuI, PPh_3 as ligands to give $\mathbf{P_1}$ (yield 63.4%) and $\mathbf{P_2}$ (yield 67.5%). The copolymers exhibit good solubility in common organic solvents such as $CHCl_3$, CH_2Cl_2, and THF. Molecular weights of the polymers were determined by gel permeation chromatography (GPC) using THF as an eluent, polystyrene as a standard. The weight-average molecular weights (M_w) of $\mathbf{P_1}$ and $\mathbf{P_2}$ are 19.9 kDa with polydispersity index (M_w/M_n) of 1.65 and 14.7 kDa with polydispersity index (M_w/M_n) of 1.68, respectively. The degrees of polymerization (DP) of $\mathbf{P_1}$ and $\mathbf{P_2}$ are 13 and 9, respectively. The results are presented in Table 1.

The chemical structures of the polymers were characterized by FT-IR, ^{1}H-NMR, ^{13}C-NMR. Figure 1 gives the FT-IR spectra of the polymers. The absorption peaks at 3442 cm^{-1} and 3439 cm^{-1} may be due to the moisture in KBr pellets. The absorption peak at 2173 cm^{-1} and 2165 cm^{-1} can be attributed to the C≡C stretching mode of the polymers $\mathbf{P_1}$ and $\mathbf{P_2}$. In addition, the strong absorption peak at 1262 cm^{-1}, 1062 cm^{-1} (for $\mathbf{P_1}$) and 1257 cm^{-1}, 1059 cm^{-1} (for $\mathbf{P_2}$) may be attributed to stretching vibration of C–O–C.

Figure 2 shows the ^{1}H-NMR spectra of the polymers. The signals at $\delta = 7.30$–7.36 ppm are for the phenyl linked to aryl ring. The peaks at $\delta = 4.06$ ppm and $\delta = 3.98$ ppm correspond to the hydrogen atoms of $-OCH_2$ linked to the thiophene ring of $\mathbf{P_1}$ and $\mathbf{P_2}$, respectively. The H signals in the alkyl side chains are observed at $\delta = 0.8$–1.6 ppm. Every peak in the ^{1}H-NMR spectra could be assigned to the corresponding hydrogen atoms of the polymers.

Thermal properties

Thermal properties of the polymers measured by thermogravimetric analysis (TGA) and differential scanning calorimetry (DSC) under a nitrogen atmosphere are summarized in Table 1. Figure 3 shows that the thermal decomposition temperatures (T_d, 95 wt% residue) of $\mathbf{P_1}$ and $\mathbf{P_2}$ are 323 and 326 °C, respectively. The relatively high onset decomposition temperatures for both polymers are indicative of high thermal stability. Apparently, the thermal stability of the polymers is adequate for their application in PSCs and other optoelectronic devices. The DSC curves of copolymers are shown in Fig. 4. The glass transition temperatures of $\mathbf{P_1}$ and $\mathbf{P_2}$ are 127 and 125 °C, respectively. The higher glass transition temperature of $\mathbf{P_1}$ is mostly because of the higher DP. It is noted that both $\mathbf{P_1}$ and $\mathbf{P_2}$ have a relatively high glass transition temperature

Scheme 1 Synthesis of the intermediate

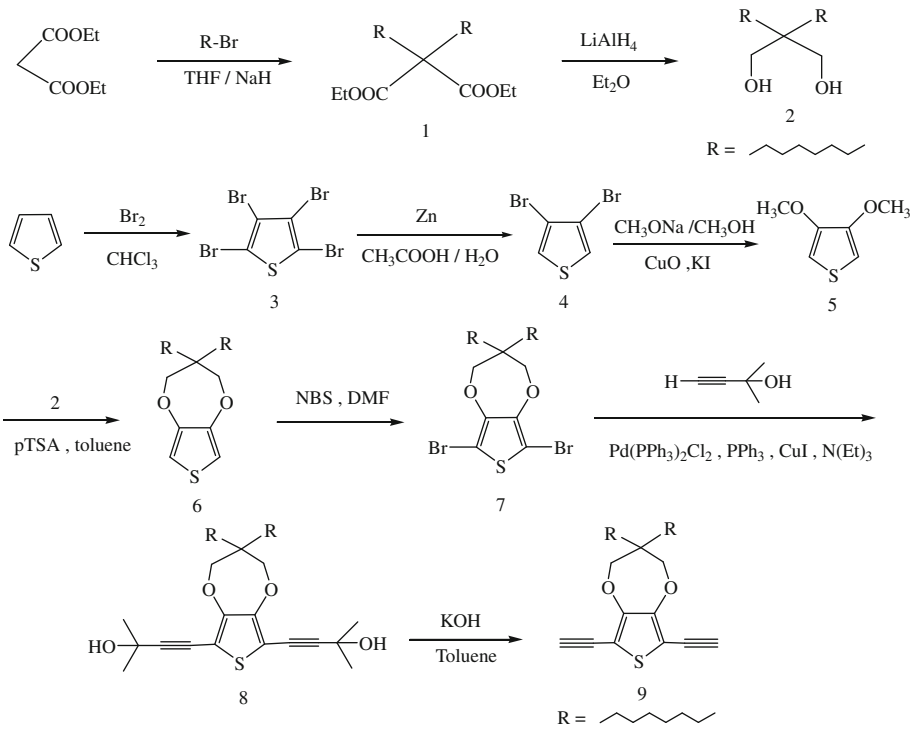

Scheme 2 Synthesis of the copolymers

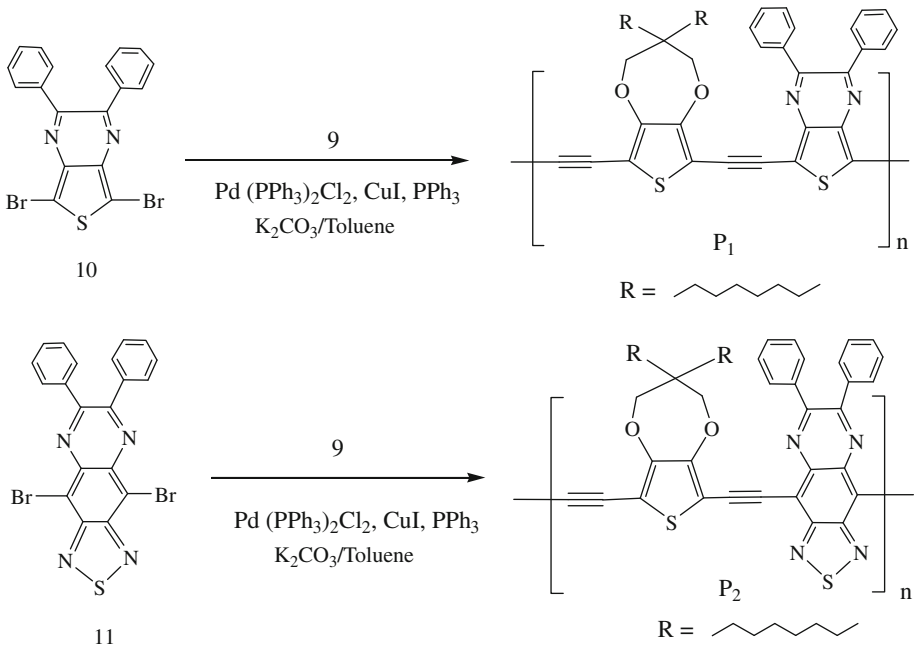

Table 1 Yield, molecular weight and thermal properties of the polymers

	Yield (%)	M_w	M_n	PDI	DP	T_d (°C)	T_g (°C)
$\mathbf{P_1}$	63.4	19,900	12,100	1.65	13	323	127
$\mathbf{P_2}$	67.5	14,700	8,700	1.68	9	326	125

PDI polydispersity index, *DP* degree of polymerzation

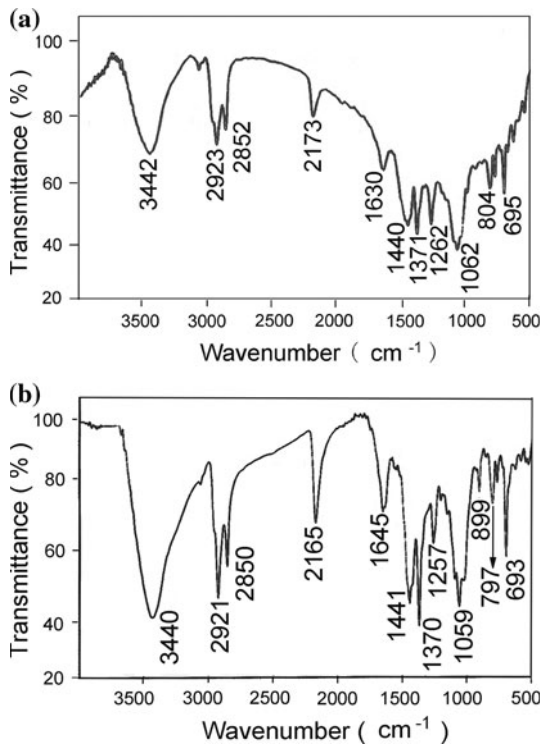

Fig. 1 FT-IR spectra of **a** the polymer $\mathbf{P_1}$; **b** the polymer $\mathbf{P_2}$

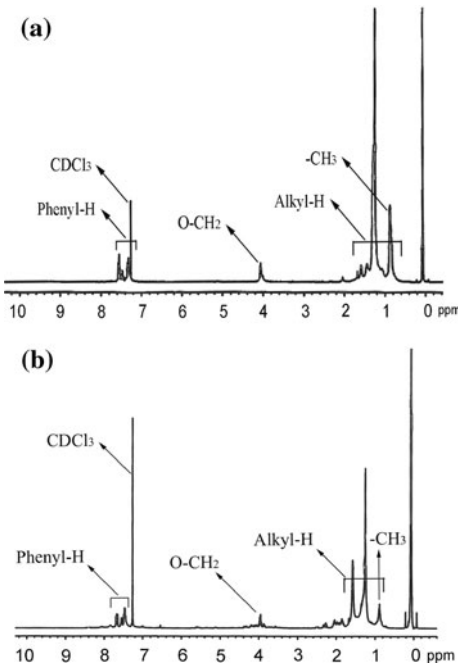

Fig. 2 ^{1}H-NMR spectra of **a** the polymer $\mathbf{P_1}$; **b** the polymer $\mathbf{P_2}$

(above 120 °C) because of the less steric hindrance occurring during polymerization, which is also essential for their photovoltaic applications.

Optical properties

UV–Vis spectra were measured both in chloroform solution and as thin films on quartz. The spectra are depicted in Fig. 5. The spectroscopic data of the polymers are

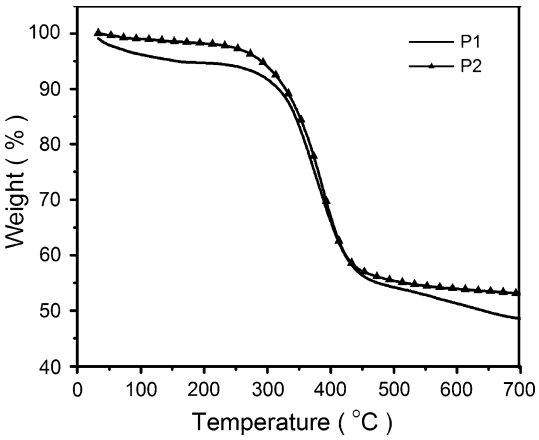

Fig. 3 TGA thermograms of the polymers

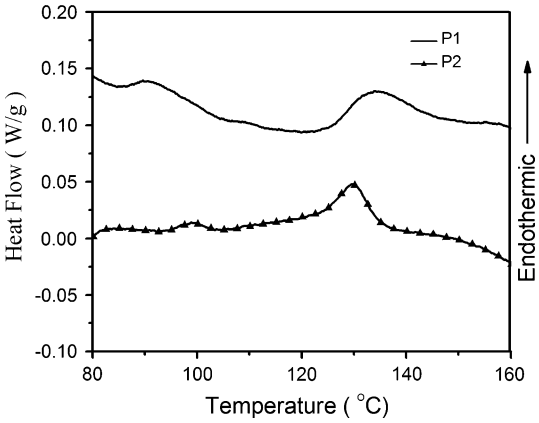

Fig. 4 DSC thermograms of the polymers

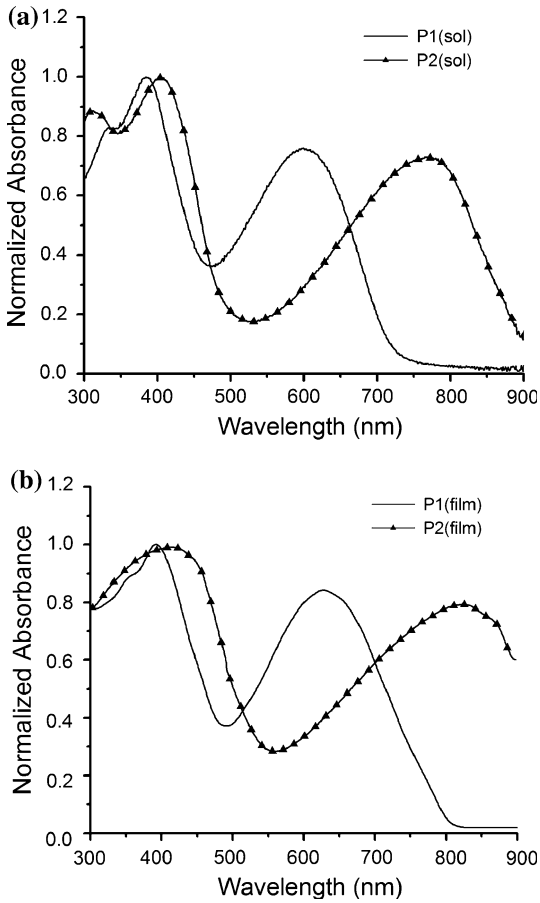

Fig. 5 UV–Vis absorption spectra of the polymers solutions in $CHCl_3$ and films on a quartz plate

summarized in Table 2. As shown in Fig. 5a, the UV–Vis spectra of $\mathbf{P_1}$ and $\mathbf{P_2}$ solution show two distinct absorption peaks: one near 385 nm ($\mathbf{P_1}$), 403 nm ($\mathbf{P_2}$) and another in 600 nm ($\mathbf{P_1}$), 766 nm ($\mathbf{P_2}$), respectively. The former peaks are assigned to $\pi \rightarrow \pi^*$ transition associated with the propylenedioxythiophene units. The absorption peaks at 600 nm and 766 nm may be assigned to the $\pi \rightarrow \pi^*$ transition of the sum of the delocalized structure resulted from the alternating donor–acceptor structure in the copolymers.

Thin films of the copolymers were spin-coated from their solution in chloroform. As shown in Fig. 5b, the absorption peak maxima of $\mathbf{P_1}$ and $\mathbf{P_2}$ are located at 385 nm, 627 nm ($\mathbf{P_1}$) and 413 nm, 825 nm ($\mathbf{P_2}$), respectively. Compared to $\mathbf{P_1}$ and $\mathbf{P_2}$ solution, the absorption peak is red-shifted by 27 nm and 59 nm in the visible spectrum. This red-shifted indicates higher coplanarity of the polymer or enhanced intermolecular electronic interaction in the solid states. The polymer $\mathbf{P_2}$ exhibited a significant absorption into the near-infrared region.

The optical band gaps (E_g^{opt}) as determined from the onset of the absorption spectra of $\mathbf{P_1}$ and $\mathbf{P_2}$ in films are 1.55 eV and 1.13 eV, respectively. The band gap of $\mathbf{P_2}$ is lower than that of $\mathbf{P_1}$, which indicates the polymer $\mathbf{P_2}$ has a stronger push–pull interaction between the diphenylthiadiazole and propylenedioxythiophene units along the polymer backbone.

Electrochemical properties

The electrochemical properties of the polymers were measured by cyclic voltammetry (CV) at room temperature. The polymer films were obtained by dip-casted onto a Pt working electrode, the positively and negatively scans were performed at a scan rate of 100 mV/s in 0.1 mol/L solution of tetra-*n*-butyl-ammonium perchlorate (*n*-Bu_4N-ClO_4) in anhydrous acetonitrile. Figure 6 shows the cyclic voltammetry of $\mathbf{P_1}$ and $\mathbf{P_2}$, Table 2 summarizes the electrochemical properties of $\mathbf{P_1}$ and $\mathbf{P_2}$. It can be seen from Fig. 6 that there are irreversible p-doping/dedoping (oxidation/rereduction) processes in the positive potential range for $\mathbf{P_1}$ and $\mathbf{P_2}$. However, for n-doping/dedoping

Table 2 Optical and electrochemical properties of the polymer $\mathbf{P_1}$, $\mathbf{P_2}$

	$\lambda_{max,sol}$ (nm)	$\lambda_{max,film}$ (nm)	E_g^{opt} (eV)[a]	$E_{onset,\ ox}$ (V)	$E_{onset,\ red}$ (V)	HOMO (eV)	LUMO (eV)	E_g^{ec} (eV)
$\mathbf{P_1}$	385, 600	385, 627	1.55	0.93	−0.69	−5.32	−3.70	1.62
$\mathbf{P_2}$	405, 766	413, 825	1.13	0.82	−0.68	−5.21	−3.71	1.50

E_g^{opt} were calculated from the absorption band edge of the copolymer films, $E_g^{opt} = 1240/\lambda_{edge}$

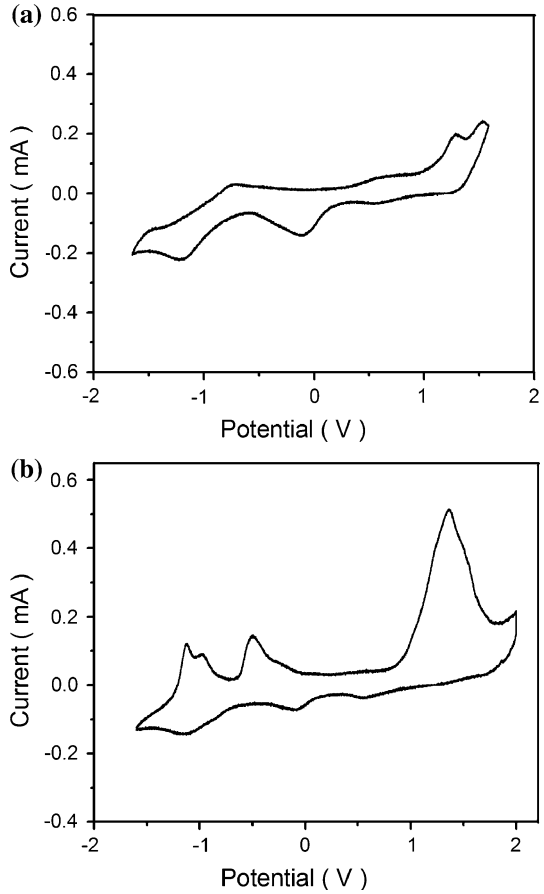

Fig. 6 Cyclic voltammogram of **a** the polymer $\mathbf{P_1}$; **b** the polymer $\mathbf{P_2}$

(reduction/reoxidation) processes in the negative potential range, $\mathbf{P_2}$ shows two reversible processes. The two reduction/reoxidation processes of copolymer $\mathbf{P_2}$ maybe due to the two oxidation positions of N atom in the 6,7-diphenyl[1,2,5]thiadiazole moiety. The first oxidation peak may be the N atom of 6,7-diphenyl substituted position, while the second oxidation peak can be attributed to the N atom in 1,2,5-thiadiazole moiety. The onsets of oxidation potential ($E_{oneset,ox}$) of $\mathbf{P_1}$, $\mathbf{P_2}$ occurred at 0.93 V, 0.82 V, respectively. The corresponding onsets of reduction potential ($E_{oneset,red}$) appeared at −0.69 V, −0.68 V, respectively. The highest occupied molecular orbital (HOMO) and the lowest unoccupied molecular orbital (LUMO) energy level of the copolymers could be obtained according to the following empirical relationships [37]:

$$I_p(\text{HOMO}) = -(E_{oneset,ox} + 4.39)\text{eV}$$

$$E_a(\text{LUMO}) = -(E_{oneset,red} + 4.39)\text{eV}$$

$$E_g^{ec} = E_{oneset,ox} - E_{oneset,red}$$

From these equations, the HOMO energy levels of $\mathbf{P_1}$, $\mathbf{P_2}$ are estimated to be −5.32 eV and −5.21 eV, respectively. The higher HOMO level of the polymer $\mathbf{P_2}$ indicates the strong intramolecular charge transfer effects [38], which is in good agreement to the push–pull interaction discussed in the optical properties section. Correspondingly, the LUMO energy levels of $\mathbf{P_1}$, $\mathbf{P_2}$ are −3.70 eV and −3.71 eV, respectively. The electrochemical band gaps (E_g^{ec}) of the polymers are calculated to be 1.62 eV and 1.50 eV. The electrochemical band gaps are larger than the optical bands probably due to the interfacial energy barrier for the charge injection [39].

Conclusions

Two novel conjugated copolymers consisting of alternating electron-rich propylenedioxythiophene and electron-deficient diphenylthenopyrazine or diphenylthiadiazole units have been synthesized by Sonogashira triple-bond coupling reaction. The copolymers exhibit good solubility in common organic solvents. The introduction of donor–acceptor units into the conjugated copolymers has achieved desirable properties of broad optical absorption and high thermal decomposition temperatures. Cyclic voltammetry experiment show that the band gaps of the copolymers are 1.62 eV and 1.50 eV, make the copolymers attractive candidates for solar cell applications.

Acknowledgements This work was supported by the key foundation of education ministry of China (20070610053) and Sichuan Province Foundation for Youths (2008JY0050). The authors also acknowledge the Analytical & Testing Center of Sichuan University for the NMR measurements.

References

1. Forrest SR (2004) Nature 428:911
2. Schmidt-Mende L, Fechtenkotter A, Mullen K (2001) Science 293:1119
3. Cheng YJ, Yang SH, Hsu CH (2009) Chem Rev 109:5868
4. Serap G, Helmut N, Niyazi SS (2007) Chem Rev 107:1324

5. Thiebaut O, Bock H, Grelet E (2010) J Am Chem Soc 132:6886
6. Zhang Y, Hau SK, Yip HL (2010) Chem Mater 22:2696
7. Goris L, Haenen K, Nesladek M (2005) J Mater Sci 40:1413. doi:10.1007/s10853-005-0576-0
8. Qiao F, Liu A, Zhou Y (2009) J Mater Sci 44:1283. doi:10.1007/s10853-009-3280-7
9. Mihailetchi VD, Xie HX, Boer BD (2006) Adv Funct Mater 16:699
10. Ma W, Yang C, Gong X (2005) Adv Funct Mater 15:1617
11. Chen LC, Godovsky D, Ingana O (2000) Adv Mater 12:1367
12. Lindgren LJ, Zhang FL, Andersson M (2009) Chem Mater 21:3491
13. Wang MZ, Xie H, Zhu JQ (2007) J Mater Sci 42:7678. doi:10.1007/s10853-007-1650-6
14. Mei JG, Svetlana NC, Vasilyeva SV (2009) Macromolecules 42:1482
15. Zhou EJ, Nakamura M, Nishizawa T (2008) Macromolecules 41:8302
16. Cai TQ, Zhou Y, Wang EG (2010) Sol Energy Mater Sol Cells 94:1275
17. Chen CH, Hsieh CH, Dubosc M (2010) Macromolecules 43:697
18. Zhang GB, Fu YY, Zhang Q (2010) Polymer 51:2313
19. Lee YK, Russel TP, Jo WH (2010) Org Electron 11:846
20. Mammo W, Admassie S, Gadisa A (2007) Sol Energy Mater Sol Cells 91:1010
21. Thompson BC, Kim YG, McCarley TD (2006) J Am Chem Soc 128:12714
22. Grenier CRG, George SJ, Joncheray TJ (2007) J Am Chem Soc 129:10694
23. Shin WS, Kim SC, Lee SJ (2007) J Polym Sci A 45:1394
24. Hammond SR, Clot O, Firestone KA (2008) Chem Mater 20:3425
25. Beaujuge PM, Vasilyeva SV, Ellinger S (2009) Macromolecules 42:3694
26. Havinga EE, Mutsaers MJ (1996) Chem Mater 8:769
27. Son JI, Hwang J, Jin SH (2009) J Electroanal Chem 628:16
28. Beaujuge PM, Ellinger S, Reynolds JR (2008) Adv Mater 20:2772
29. Mishra SP, Krishnamoorthy K, Sahoo R (2004) J Polym Sci A 43:419
30. Reeves BD, Grenier CRG, Argun AA (2004) Macromolecules 37:7559
31. Nielsen CB, Bjornholm T (2005) Macromolecules 38:10379
32. Kenning DD, Mitchell KA, Calhoun TR (2002) J Org Chem 67:9073
33. Cheng KF, Liu CL, Chen WC (2007) J Polym Sci A 45:5872
34. Zoombelt AP, Fonrodona M, Wienk MM (2009) Org Lett 11:903
35. Qian G, Zhong Z, Luo M (2009) J Phys Chem C 113:1589
36. Susumu K, Duncan TV, Therien MJ (2005) J Am Chem Soc 127:5186
37. Bredas JL, Silbey R, Boudreaux DS (1983) J Am Chem Soc 105:6555
38. Tsai JH, Chueh CC, Lai MH (2009) Macromolecules 42:1897
39. Chen ZK, Huang W, Wang LH (2000) Macromolecules 33:9015